Preamble Structure for fast Acquisition and Equalization of QAM Signals

fred harris, San Diego State University
fred.harris@sdsu.edu

Chris Dick, Xilinx Corporation
chris.dick@xilinx.com

Abstract

A receiver must estimate a number of essential unknown valued signal parameters from a received signal in order to demodulate the information in that signal. These parameters include, signal strength, carrier frequency and phase, sample time frequency and phase, and channel gain and phase distortion terms responsible for inter-symbol interference. These parameters can be extracted from a preamble training signal designed for their fast acquisition. This paper describes the signal structure and the signal processing required to rapidly estimate these parameters and how they are incorporated in appropriate processing block to support the demodulation functions.

Introduction

Modern digital radio systems transmit a sequence of known bandwidth limited baseband wave shapes at a nominal symbol rate. The amplitude, phase, or phase slope of these wave shapes are selected from a list of symbol amplitudes called the signaling alphabet. The selection process is a mapping between binary input sequences and output alphabet characters which may incorporate the memory of earlier input sequences or output characters. The spectrum of the baseband signal is translated or up-converted to a nominal center frequency by a complex heterodyne operation which results in a narrowband time signal exhibiting amplitude and phase modulation of the carrier centered signal. This modulated and translated signal structure, s(t), is shown in (1).

$$\begin{aligned} s(t) &= \mathrm{Re}\{[\sum_n I_n h(t-nT)]e^{j\omega_c t}\} \\ &= \mathrm{Re}\{R(t)e^{j\theta(t)}e^{j\omega_c t}\} \end{aligned} \tag{1}$$

The narrowband signal is coupled by an antenna to the ether which launches a propagating wave into the transmission medium. The signal experiences a number of modifications in its journey from the modulator in its transmitter to the demodulator in its receiver. These include linear distortion caused by analog filters in the transmitter and receiver and constructive and destructive interference due to multipath channel components. The signal collected at the receiver exhibits other unknown parameters due to the channel which include unknown attenuation, unknown time offset due to propagation delay, unknown frequency offset due to velocity differences between transmitter and receiver platforms as well as frequency offsets and drifts due to manufacturing tolerance, aging, and temperature differences, and additive noise due to the receiver's low noise amplifier. In addition to the linear distortion effects there are non linear effects which include non uniform gain of the power amplifier at the transmitter output stage and third order Intermodulation between nearby channels in the low noise amplifier at the receiver input stage. The received signal structure r(t) with linear channel effects is shown in (2).

$$\begin{aligned} r(t) = \\ \mathrm{Re}\{[A(t,\tau) * R(t-\tau)e^{j\theta(t-\tau)}]e^{j(\omega_c+\Delta\omega)(t-\tau)}\} + n(t) \end{aligned} \tag{2}$$

For successful demodulation of the received signal, the demodulator must form reliable estimates of the frequency offset $\Delta\omega$, the time offset τ, the channel attenuation $E\{A(t,\tau)\}$, and the channel model $A(t,\tau)$. For optimal processing the demodulator should also estimate E_b/N_0 or SNR, and for practical processing, the demodulator must estimate time of arrival to disable the squelch and enable the demodulator detection algorithms. Consequently, a modern modulator and demodulator have the form shown in figure 1. We see here the asymmetry between the modulator and demodulator. The demodulator requires the use of a number of processing blocks to estimate the various unknown parameters. As we will see, some of the parameters are estimated concurrently and some are estimated sequentially.

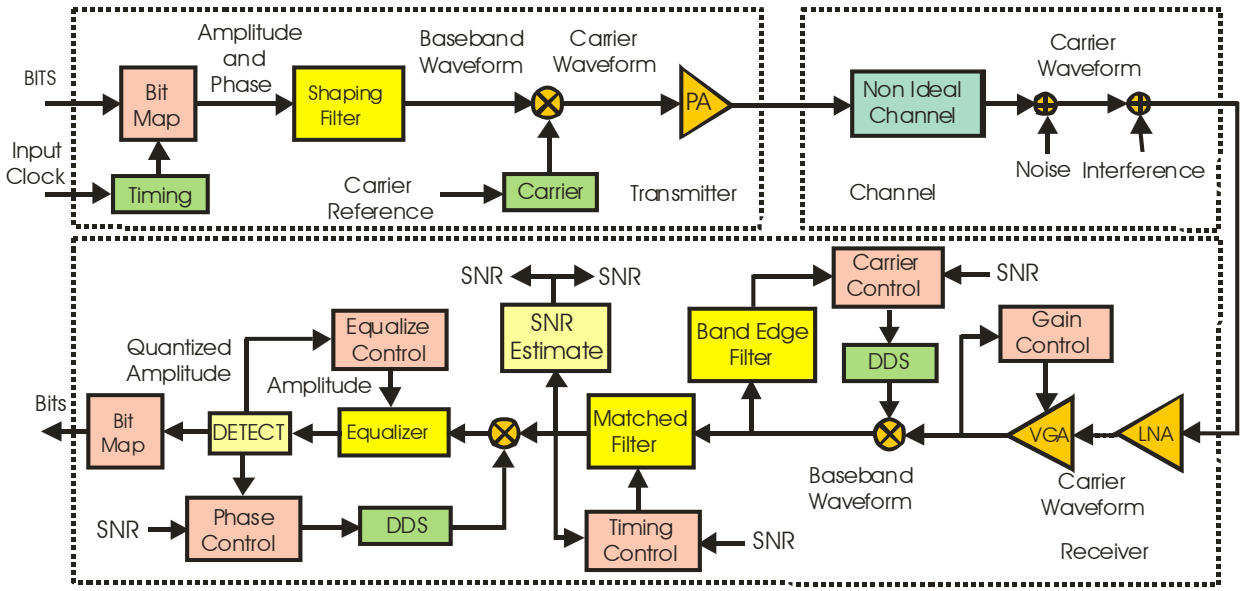

Figure 1. Modern Digital Modulator and Demodulator

Preamble Structure: First Segment

The target design task described in this paper was the design of a preamble for a burst modem that would acquire signal edge detection, AGC, carrier frequency and phase offset, time alignment, and equalization in less than 100 symbol intervals. We present here the design and performance of the initial design which has been significantly improved upon in subsequent tuning efforts. The preamble is composed entirely of QPSK constellation points shaped by the standard SQRT Nyquist shaping filter with 25% excess bandwidth. A design requirement specified the input sample rate for the modem to be 16 samples per symbol.

The first segment of the preamble was designed to accomplish 5-tasks. These are signal detection, AGC, carrier frequency and phase lock, and timing acquisition, and time tag. This first segment, called the short preamble, is a sequence of two QPSK constellation sequences consisting of 24 constellation points alternating from the upper right (1+j1) to the lower left (-1-j1) corners of the unit square. The alternating signs of the both I and Q components makes the envelope of this time sequence has the appearance of a sine wave. The 24 symbol sine wave like sequence is repeated with a sign change after the first 24 symbol sequence. This sign change is detected and used as a time tag within the preamble by its associated state machine. The two time series corresponding to this segment of the preamble is seen in the interval between samples 10 to 68 in figure 2. At 16-samples per symbol, it takes 32 samples to span one cycle of the equivalent sine wave formed by successive alternating sign symbols.

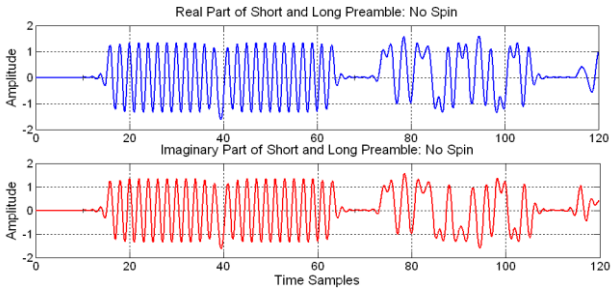

Figure 2. Real and Imaginary Parts of Fast Preamble

A trivial transformation of the identical I and Q components of the sine wave like signal is obtained by delaying the signal 8-samples, or a quarter cycle, and forming the analytic signal as a quadrature sum as shown in (3). The quarter cycle time delay of the sine wave offers the 90° phase shift of a Hilbert Transform.

$$\begin{aligned} dat\_HT=\{&[dat(1{:}n\_len)\ \ zeros(1,8)]+\\ &j*[zeros(1,8)\ \ dat(1{:}n\_len)\ ]\} \end{aligned} \tag{3}$$

The analytic signal version of the sine wave converts the oscillating 45° phase trajectory of the matching I-Q pair to a rotating phase trajectory of a standard phasor. When there is frequency offset, the oscillating phase trajectory is seen to slowly rotate its trajectory line while the analytic signal version is a con-

stant amplitude phasor spinning at the nominal rate of 32-samples per cycle plus the incremental rate due to a frequency offset. The phase trajectories for these two conditions are seen in figure 3. The constant envelope of the analytic signal makes it uniquely qualified to guide the AGC loop, the signal detection cross and auto correlation loops, the frequency offset detector and the time tag detector. A partial block diagram of Hilbert transform process and associated AGC Loop and auto and cross correlator detectors is shown in figure 4. The cross correlation between input and 64-sample delayed input spans a two cycle interval of the sine wave section of the preamble. The ratio of cross to auto correlation presents an excellent statistic for preamble signal detection. This ratio detection can be seen in the lower sub plot of figure 5. Similarly, cross correlation over a quarter cycle interval is used to detect the sign reversal boundary in the short preamble. This correlation spike can be seen in the lower subplot of figure 6. The upper subplot of figure 6 shows the AGC profile and the gating time tags launched by the detections of the correlation ratio and of the sign reversal correlation peak. These gating functions identify the intervals spanned by the short and by the long preamble and guide the state machine processing the preamble signal.

In parallel with the AGC loop processing and the auto and cross correlations of the Hilbert Transformed sine wave samples of the non Hilbert transformed input sine wave are tested and compared with the previous samples to identify the sample nearest the peak value. Due to the alternating signs of successive data samples in the short preamble, the peak sample values correspond to the timing sample. The angle of the I-Q ordered pair at this sample time should be located at the two corner constellation point 1+j1 and -1-j1. The error angle between the observed ordered pair and the two reference points is measured and is driven to zero by a PLL controlled a Direct Digital Synthesizer (DDS). Figure 7 shows the I-Q components at input and output of phase and timing acquisition processes. Note that by the time the short preamble sign reversal has been detected AGC, Timing, and Phase lock have been accomplished.

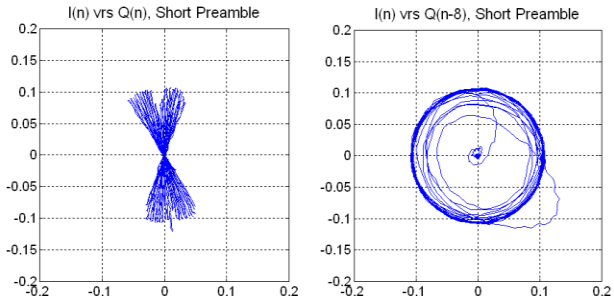

Figure 3 I-vs.-Q for Matching I-Q Sine Wave and Hilbert Transformed by time Delay Sine Wave

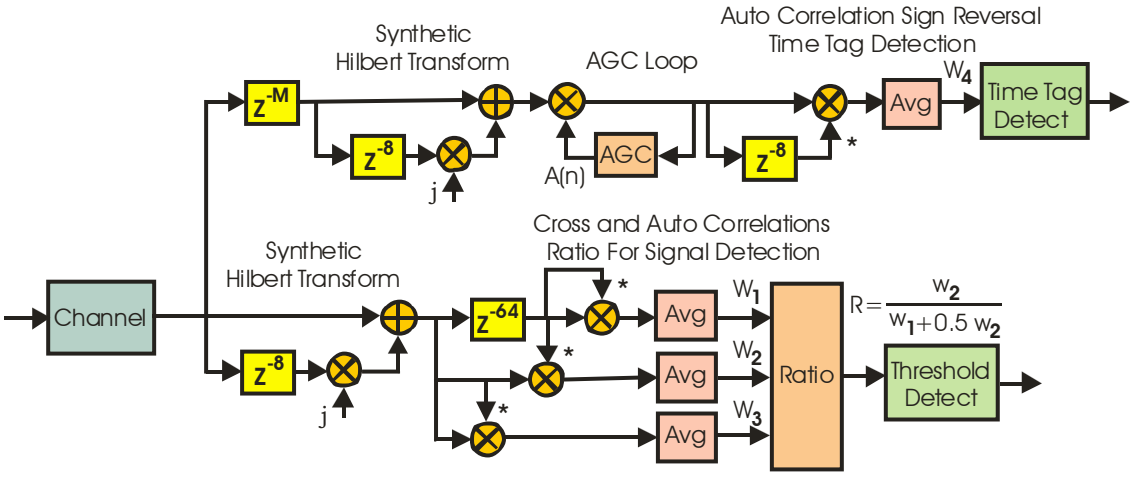

Figure 4. Partial Block Diagram of Short Preamble Detection Processing: Hilbert Transforms, AGC, and Cross Correlation $E\{A(n)d(n)A(n-8)d^{*}(n-8)\}$ for Sign Reversal Detection and Ratio of Cross-Correlation $E\{d(n)d^{*}(n-64)\}$ to Auto-Correlation $E\{d(n-64)d^{*}(n-64)\}$ for Preamble Detection.

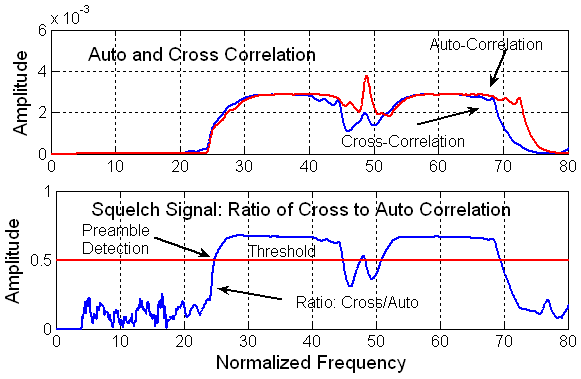

Figure 5. Auto and Cross Correlation and Ratio crossing Threshold To time tag start of Preamble.

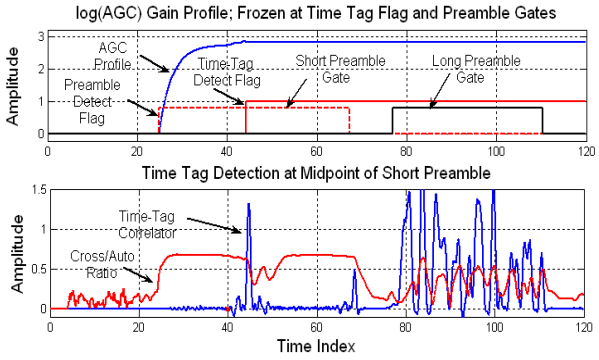

Figure 6. AGC Profile, Detection Time Tags, Short and Long Signal Gates and Short Cross Correlation for Sign Reversal Detection.

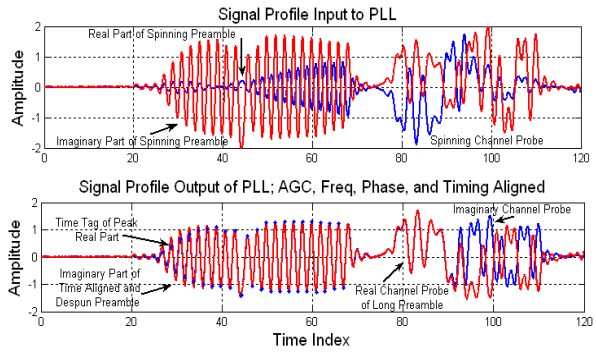

Figure 7. Spinning I-Q Components at Output of AGC Process and at Input and Output of Phase and Timing Acquisition Processes.

Preamble Structure: Second Segment

The second segment of the preamble contains a pair of 32-chip complementary code spreading sequences. The two sequences are formed by the recursive relationship shown in (4).

$$[A_{n+1}]=[A_n\ B_n],\ [A_0]=1$$
$$[B_{n+1}]=[A_n\ \bar{B}_n],\ [B_0]=1 \qquad (4)$$

The two sequences $[A_n]$ and $[B_n]$ have de-spreading matched filter responses with a single main lobe and with opposing polarity side-lobes. Due to their cancelling side lobes, the sum of the two matched filter output responses is a single offset impulse 2N δ(n-N). When the complementary codes are delivered to their matched filters through the channel, the summed responses is the channel impulse response. The complementary de-spreading matched filters operate at 2-samples per symbol. Figure 8 shows the matched filter responses and their sum, the channel impulse response. This impulse response is resampled to 1-sample per symbol and is processed by a MMS approximation to the Normal equation to compute the weights of a 15-tap tapped delay line equalizer. Figure 9 shows the channel response, the equalizer impulse response, and their convolution. The solution of the Normal equation is inserted as the initial weights of an LMS equalizer that processes signal payload after the preamble.

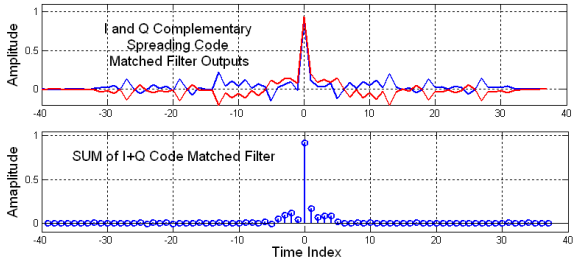

Figure 8. Matched Filter Responses of I-Q Complementary Codes and their Sum Sampled at Symbol Rate

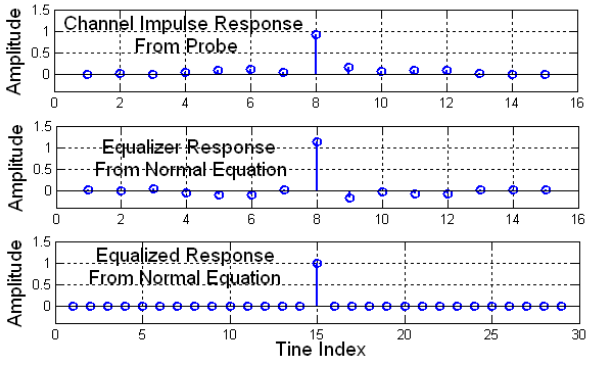

Figure 9 Channel Impulse Response from Complementary Code Probe, Equalizer Impulse Response formed from Normal Equation and Equalized Response.

Figure 10 shows the response of the second segment of the preamble along with the start of 16-QAM signal payload following the preamble after these signals have been passed through the equalizer initialized with the response formed from the complementary code channel probe. Figure 11 shows the impulse response of the channel used in this simulation and figure 12 shows the 16-QAM constellation points input to and output from equalizer along with a 2-sample per symbol eye-diagram formed from the equalized time series.

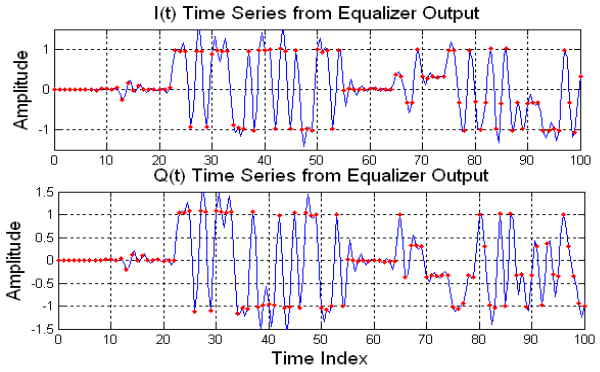

Figure 10. Equalized Response of I-Q components Formed from Channel Probe.

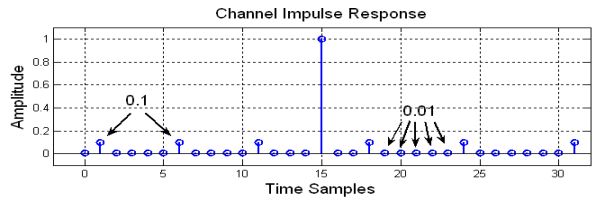

Figure 11. Channel Impulse Response

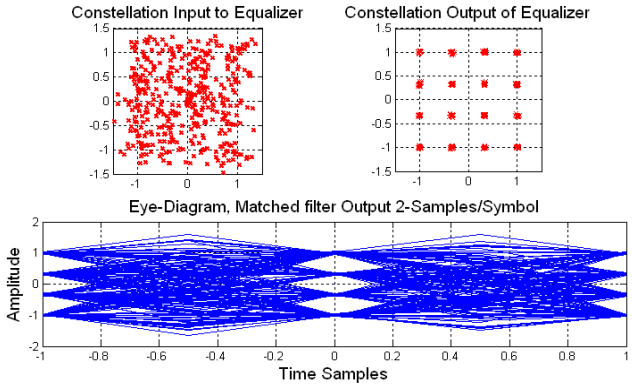

Figure 11. 16-QAM Constellation at Input and Output of Equalizer and 2-Sample per Symbol Eye Diagram of Equalized Response.

Closing Comments:

We have described the structure and the signal processing of a preamble designed for fast acquisition of a QAM signal with targeted preamble length of less than 100 symbols. We have presented a number of figures to demonstrate typical wave shapes formed by the signal processing operations. The signal structure contained zero valued gaps between signal segments which were included for ease of debugging the processing code and for clarity of illustration. These gaps are to be removed in the actual deployment. The preamble was used to acquire squelch, AGC, Timing, Carrier, and Channel parameters. The acquisition initialized and operated their associated loops during the preamble. At the end of the preamble interval, the system state machine enables a control handover to the standard tracking modes based on data directed loop operation.

References:

[1]. Steve Gardner, “Burst Modem Design Techniques, Part 1”, Communication System Design, Volume 5, Number 7, July 1999.

[2]. Jingxin Chen, “Carrier Recovery in Burst Mode 16-QAM”, Thesis, University of Saskatchewan, 2004.

[3]. Yougje Kim, Yongtae Kim, Yongwook Lee, Wangrock Oh, and Whanwoo Kim, “Synchronization and Channel Equalization for Upstream Cable Modem”, International Symposium Consumer Electronics, ISCE-2008, 14-16 April 2008.

[4]. Mark Engels, “Wireless OFDM Systems”, Kluwer Academic Publishers, 2002.

[5]. John Barry, Edward Lee, and David Messerschmitt, “Digital Communications”, 3-rd Ed., Springer, 2003.

[6]. fred harris, and Chris Dick, “A Versatile Filter Structure to Generate and Compress Binary and Polyphase Complementary Spreading Codes”, Software Defined Radio Conference, SDR-2004, Phoenix, AZ, 15-17 November 2004.

[7]. David Lynch, “Introduction to RF Stealth”, Scitech Publishing, Raleigh, NC, 2004